



Platinum supported catalysts for carbon monoxide preferential oxidation: Study of support influence

R. Padilla^{a,*}, M. Benito^{a,b}, L. Rodríguez^a, A. Serrano-Lotina^a, L. Daza^a

^a Instituto de Catálisis y Petroleoquímica (CSIC), C/Marie Curie 2, Campus Cantoblanco, 28049 Madrid, Spain

^b Centro de Investigaciones Energéticas Medioambientales y Tecnológicas (CIEMAT), Av. Complutense 22, 28040 Madrid, Spain

ARTICLE INFO

Article history:

Received 14 October 2008

Received in revised form 3 December 2008

Accepted 22 December 2008

Available online 29 January 2009

Keywords:

Catalyst
Preferential oxidation
Fuel processor
Fuel cell
Hydrogen

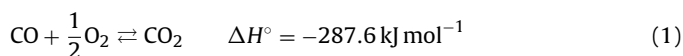
ABSTRACT

The aim of this work is to study the influence of the addition of different oxides to an alumina support, on surface acidity and platinum reducibility in platinum-based catalysts, as well as their effect on the activity and selectivity in CO preferential oxidation, in presence of hydrogen. A correlation between surface acidity and acid strength of surface sites and metal reducibility was obtained, being Pt-support interaction a function of the acid sites concentration under a particular temperature range. In platinum supported on alumina catalysts, CO oxidation follows a Langmuir–Hinshelwood mechanism, where O₂ and CO compete in the adsorption on the same type of active sites. It is noteworthy that the addition of La₂O₃ modifies the reaction mechanism. In this case, CO is not only adsorbed on the Pt active sites but also on La₂O₃, forming bridge bonded carbonates which leads to high reactivity at low temperatures. An increase on temperature produces CO desorption from Pt surface sites and favours oxygen adsorption producing CO₂. CO oxidation with surface hydroxyl groups was activated producing simultaneously CO₂ and H₂.

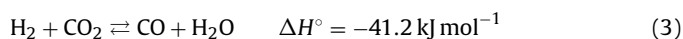
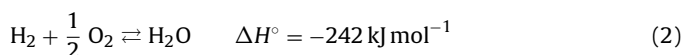
© 2009 Elsevier B.V. All rights reserved.

1. Introduction

In the transition to hydrogen economy, the development of processes that produce hydrogen from fossil fuels has a remarkable worldwide interest. In these processes hydrogen is usually obtained by steam reforming or partial oxidation in combination with the water gas shift reaction. The resulting gases contain about 1% of CO, which needs a further reaction stage in order to obtain a CO free stream. The aim of carbon monoxide preferential oxidation, denoted as COPROX (1), is to diminish CO concentration at ppm levels by means of selective oxidation with oxygen, producing CO₂ in hydrogen presence, without H₂ consumption.



It is necessary to optimize operation conditions such as temperature, O₂/CO ratio and catalyst mass/stream flow ratio, in order to minimize the H₂ oxidation (2) or the reverse water gas shift reaction (3) which could take place simultaneously or consecutively, decreasing consequently hydrogen production efficiency.



Catalysts used for COPROX processes in presence of H₂ reported in the literature can be classified in three types [1,2]: (1) gold catalysts supported on one or two of the following oxides: α-Fe₂O₃, TiO₂, CoO_x, NiO_x, Mg(OH)₂, CeO₂, SnO₂, MnO_x, γ-Al₂O₃ and ZnO; (2) catalysts based on metal oxides, such as Cu, Ce, Mn, Co and Ni alone or combined with others [3,4]; (3) noble metal catalysts (Pt, Ir, Pd, Ru or Rh) supported on CeO₂, Al₂O₃, SiO₂, SiO₂–Al₂O₃, La₂O₃, MgO, CeO₂, Ce_xZr_(1-x)O₂, TiO₂, mordenite and active carbon [5,6].

The articles found in literature related to gold catalysts show results where catalysts usually operate in the temperature range 50–100 °C, they are fed with CO, O₂ and an inert gas (N₂ or He) using a O₂/CO ratio between 1 and 20/1. Some studies of H₂ addition (5–75%) were reported, being CO₂ and H₂O addition found less frequently [7]. At low temperatures, highly dispersed gold particles over an oxide support showed high activity and selectivity. However, the catalyst activity strongly depended on the preparation method [8–10].

In the case of type two catalysts, catalyst are operated at temperatures between 80 and 160 °C, they are fed with CO, O₂, H₂ and an inert gas, with an O₂/CO ratio range between 1/1 and 10/1 and a H₂ concentration of 40–50%, without CO₂ addition. Finally, type three catalysts are operated in a wide temperature range (80–300 °C) and they are fed with 1% CO, 1–4% O₂, 30–70% H₂, 10–20% CO₂ and 10–20% H₂O.

Platinum supported catalysts are solid candidates to be used in a fuel processor, due to their ability to operate at high temperatures and their high resistance to deactivation by CO₂ or H₂O presence. Many efforts have been made to improve the activity and selectivity.

* Corresponding author. Tel.: +34 91 5854793; fax: +34 91 5854760.
E-mail address: ritapadilla@icp.csic.es (R. Padilla).

ity of Pt catalyst used in COPROX process. For example, dopants and promoters have been added to Pt/Al₂O₃ catalysts [11,12], in order to minimize the adsorption of CO on Pt, which blocks the O₂ adsorption sites (oxygen adsorption is the rate-determining step), making CO oxidation difficult. CO oxidation rate seems to decrease with the increase on the strength of CO–Pt interaction.

The goal of this work is to study the influence of the addition of support modifiers on the activity and selectivity of platinum supported on alumina-based catalysts. The effect on acidity, reducibility and the CO adsorption mechanism was also determined.

2. Experimental

2.1. Catalysts preparation

Four platinum-based catalysts were prepared by impregnation in dissolution method. They were supported on alumina (PtAc) and alumina with 20 wt.% SiO₂ (PtSiA), 50 wt.% MgO (PtMgA) and 3 wt.% La₂O₃ (PtLaA), H₂ PtCl₆·6H₂O (Degussa) was the precursor salt used for the active phase. The nominal platinum concentration was 1 wt%. After drying in air (110 °C, 12 h), the catalysts were calcined in air at 500 °C for 2 h.

2.2. Characterization

Specific surface area (S_{BET}) was measured by N₂ adsorption at 77 K in a *Micromeritics Asap 2010* apparatus. Prior to measurement, the sample was out-gassed at 140 °C during 24 h on a *Vacprep 061 Lb Micromeritics* equipment.

XRD patterns were obtained on powder samples in a diffractometer *Seifert XRD 3000P* at 2 θ range 2–100°, using Cu K α radiation ($\lambda = 1.540598 \text{ \AA}$), removing K α radiation by a nickel filter, with a 0.05° s⁻¹ scanning and a accumulation time of 2 s. Crystalline phases were identified comparing the patterns obtained with Joint Committee on Powder Diffraction Standards 1971 data base.

The acidity and the acid strength of the support sites were determined by temperature programmed NH₃ desorption, performed in a *Micromeritics Asap 2010*. Samples were out-gassed in a *Vacprep 061 Lb Micromeritics* apparatus.

Temperature programmed reduction (TPR) tests were performed with 10% H₂–90% N₂ (50 cm³ min⁻¹) in the temperature range of 25–700 °C. Tests were performed in a micro-activity equipment, *PID Eng&Tech* being hydrogen consumption analyzed by an *Agilent 6890N* chromatograph equipped with TCD and FID detectors.

Metal dispersion (D_{M}) defined as metal particles present on the surface of the catalyst vs. total amount of metal contained in the catalyst, was determined from H₂ dynamic chemisorption measurements carried out in a *Pulse Chemisorb 2700 Micromeritics* apparatus. Samples were reduced under pure H₂ and they were further out-gassed under argon flow. It is well-known the mechanism of hydrogen adsorption on Pt sites. Considering a dissociative adsorption, the adsorption stoichiometry considered to calculate platinum dispersion was H_{ad}:Pt_s = 1:1. Therefore, the exposed platinum surface was calculated from the hydrogen consumption taking into consideration that physisorption on the metal and the support are negligible.

CO chemisorption isotherms were obtained in a volumetric apparatus at 25 °C up to 180 Torr. CO TPD (temperature programmed desorption) experiments were performed to obtain information about surface active sites distribution. A 0.15 mg powder catalyst sample was placed in an adsorption reactor and was submitted to a reduction pre-treatment. TPD experiments were carried out by increasing temperature rate of 10 °C min⁻¹ from room temperature up to 500 °C and maintaining at 500 °C for 10 min. Composition of desorbed gases was measured by a mass spectrometer *Pfeiffer Vacuum GMBH D 35614* connected to a vacuum volumetric apparatus.

2.3. Activity tests

Catalytic tests were carried out in a *Microactivity Reference PID Eng&Tech* equipment. The catalytic bed was formed by a catalyst sample and an inert diluter (SiC) in a 1:4 weight ratio. Prior to the catalytic measurement, the catalysts were reduced *in situ* with pure H₂ flow of 100 cm³ min⁻¹ for 1 h at 500 °C. Catalytic samples were submitted to a temperature scan from 25 to 255 °C. The reaction mixture composition was 41% H₂, 1% CO and 1% O₂ (N₂ balance) being the W/F ratio 0.09 g_{cat} s cm⁻³. Oxygen concentration fed was twice the stoichiometric ($\lambda = 2$, $\lambda = 2[\text{O}_2]/[\text{CO}]$).

W/F ratio (4) is defined as the catalyst mass (W_{cat}) divided by the gas flow fed (F_{T}):

$$\frac{W}{F} (\text{g}_{\text{cat}} \text{ s cm}^{-3}) = \frac{W_{\text{cat}}}{F_{\text{T}}} \quad (4)$$

Catalytic activity denoted as X_{CO} is defined in the following equation:

$$X_{\text{CO}}(\%) = \left(\frac{([\text{CO}]_{\text{in}} - [\text{CO}]_{\text{out}})}{[\text{CO}]_{\text{in}}} \right) \cdot 100 \quad (5)$$

where $[\text{CO}]_{\text{in}}$: mol of CO in reactor input, $[\text{CO}]_{\text{out}}$: mol of CO in reactor output.

Selectivity to CO₂, defined as the oxygen converted to produce CO₂ vs. oxygen converted to produce H₂O, was calculated using an oxygen mass atom-gram balance in each chromatograph analysis (Eq. (6)):

$$S_{\text{CO}_2}(\%) = \left(\frac{2 [\text{CO}_2]}{2 [\text{CO}_2] + [\text{H}_2\text{O}]} \right) \cdot 100 \quad (6)$$

The product reaction analysis was performed with an on-line *Agilent 6890N* chromatograph, equipped with TCD and FID detectors.

3. Results and discussion

3.1. Characterization

Texture parameters for each support and catalyst considered, calculated from isotherms, are compiled in Table 1. The support with SiO₂ (SiA) showed the highest surface area (390 m² g⁻¹), followed by LaA and MgA (supports with La₂O₃ and MgO, respectively) (148 and 140 m² g⁻¹, respectively), and finally by alumina (Ac) (93 m² g⁻¹). After the impregnation of Pt, surface area decreased, especially for PtSiA catalyst. A decrease in pore diameter and an increase in pore volume are also observed in PtAc. However, in

Table 1
Textural features of supports and catalysts: BET surface area (S_{BET}), pore diameter (d_{pore}), pore volume (V_{pore}).

Support	S_{BET} (m ² g ⁻¹)	d_{pore} (nm)	V_{pore} (cm ³ g ⁻¹)	Catalyst	S_{BET} (m ² g ⁻¹)	d_{pore} (nm)	V_{pore} (cm ³ g ⁻¹)
Ac	93.2	48.6	0.285	PtAc	92.3	22.3	0.710
MgA	140.6	10.4	0.505	PtMgA	130.8	8.8	0.231
SiA	390.3	6.8	0.772	PtSiA	351.6	6.1	0.756
LaA	148.2	10.4	0.505	PtLaA	141.2	10.3	0.496

Table 2
Supports acidity and acid strength (A.S.) by NH₃ chemisorption at 30 °C.

Support	NH ₃ chemisorbed ($\mu\text{mol g}^{-1}$)	Acidity (10^{20} acid sites g^{-1})	A.S. (%)		
			100 (°C)	200 (°C)	300 (°C)
Ac	4170	2.51	100	91.5	84.7
MgA	2880	1.73	43.2	0	0
SiA	7950	4.79	77.9	60.9	0
LaA	3560	2.14	99.8	60.2	29.5

PtMgA catalyst pore volume decreased, remaining the same for the other catalysts.

By X-ray diffraction, the presence of $\delta\text{-Al}_2\text{O}_3$ (47–1770) and $\gamma\text{-Al}_2\text{O}_3$ (47–1308) phases were identified in Ac support as well as in PtAc catalyst. In MgA support and PtMgA catalyst, the highest intensity bands, that could be ascribed to $\gamma\text{-Al}_2\text{O}_3$ (47–1308), are shifted to lower diffraction angles. This fact can be due to the insertion of MgO in the Al_2O_3 structure, forming $\text{Al}_2\text{Mg}_{1-x}\text{O}_{4-x}$ species, though it was not detected by X-ray analysis. In SiA support and in PtSiA catalyst, the main diffraction peaks can be ascribed to $\gamma\text{-Al}_2\text{O}_3$ (47–1308) and $\text{Al}_{1.9}\text{Si}_{0.06}\text{O}_{2.95}$ (37–1483). In the diffractograms of LaA and PtLaA the peaks of higher intensity can be ascribed to $\gamma\text{-Al}_2\text{O}_3$ (47–1308 and 48–367). The absence of peaks ascribed to lanthanum compounds should not be attributed to the low La_2O_3 content (3%). It can be explained by the high dispersion level of La on the alumina surface that can be amorphous or microcrystalline. At surface concentrations lower than $8.5 \mu\text{mol m}^{-2}$, La_2O_3 forms a 2D layer invisible to X ray [13], being the surface concentration in the PtLaA catalyst we prepared, $0.26 \mu\text{mol m}^{-2}$, which is lower than the value reported previously.

In addition, diffraction peaks ascribed to Pt species (ref. 75–1059, PtO_2) are not detected, what can indicate a high dispersion rate of Pt over the supports. It is important to note that we worked at detection limit levels (1%), being difficult to discriminate in crystalline diameters lower than 5 nm.

Chemisorption measures with NH₃ are compiled in Table 2. The acidity order of the supports was $\text{MgA} < \text{LaA} < \text{Ac} < \text{SiA}$. The acid strength (A.S.) is connected with the desorption temperature of the basic centres, defined as the NH₃ centres that are not desorbed after being out-gassed at 100, 200 and 300 °C. The acid strength order of the supports was $\text{MgA} < \text{SiA} < \text{LaA} < \text{Ac}$. So, Ac was the support that shows the highest acid strength.

In TPR tests (Fig. 1), two peaks, corresponding to the Pt reduction, were identified. In PtAc, PtSiA and PtLaA catalysts, the first

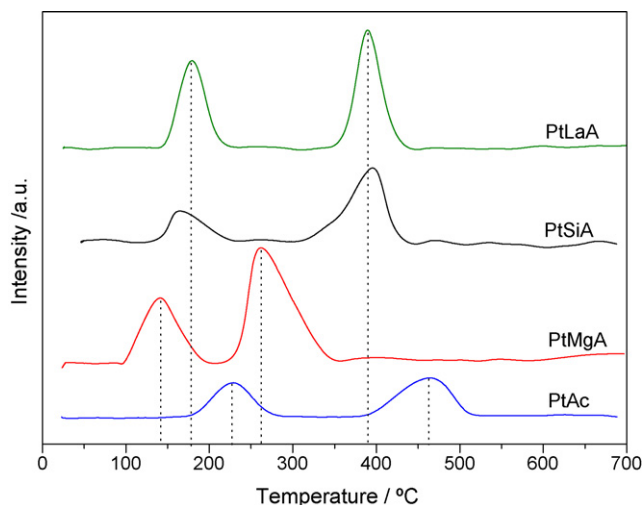


Fig. 1. Temperature programmed reduction experiments (TPR) performed with the catalysts PtAc, PtMgA, PtSiA, PtLaA.

peak was observed between 150 and 220 °C and the second one between 390 and 460 °C. At 250 °C, the reduction of most part of PtO_x species happens. The second peak (430 °C) is the result of the reduction of the PtO_x species that shows a stronger interaction with the support [14–16]. Comparing the Pt reducibility order with the acid strength of the support, we can affirm that as the acid strength of the supports decreases, the catalyst is more easily reducible (Table 2). Therefore, the interaction between Pt and the support depends on the acid centres concentration.

By hydrogen pulsed chemisorption, the exposed metallic surface was determined. All the catalysts showed a high dispersion (Table 3), with the exception of PtMgA, what confirms the relation between the Pt dispersion in the catalysts surface and the acid strength of the supports. PtMgA catalyst, with the lowest acidity and acid strength, is the one which showed the lowest Pt dispersion and consequently the highest particle size, though it has a high surface area. PtLaA catalyst is the one with the highest dispersion (85.9%), because La_2O_3 works as a stabilizer in the distribution of the metallic particles, leading to a lower crystal size [17]. As lanthanum strongly modifies the morphology of alumina support, it provides an increased number of nucleation sites for metals during the synthesis of the catalyst, leading to an enhancement of the initial repartition and dispersion of the metallic phase [18].

In CO TPD tests (Fig. 2), the profile of the desorbed species vs. temperature (25–500 °C at a temperature rate of $10^\circ\text{C min}^{-1}$ (a), and isotherm period at 500 °C (b)), is shown for each of the catalysts considered. They show wide desorption peaks which means some heterogeneity in the adsorption sites. This heterogeneity is a result of different activation energies for desorption which are a function of the surface coverage of CO on the Pt surface and depends on the size distribution of the Pt particles [19]. Two peaks ascribed to CO desorption can be differentiated, one at low temperature (200–260 °C) and the other at high temperature (400–500 °C), taking place the highest intensity desorption at low temperature [20,21]. CO desorption at low temperatures is associated with the linear CO adsorption over small Pt particles. CO desorption at high temperatures can be ascribed to bridge bonded CO species [22,23], or with the species adsorbed in more inaccessible sites, what would need a higher temperature to be desorbed [22,24]. In PtAc and PtSiA catalysts, CO desorption (Fig. 2i and iii) began at higher temperatures than in the case of PtMgA and PtLaA catalysts (Fig. 2ii and iv), what can be related with the highest acidity of Ac and SiA supports [25]. In all cases, in the isotherm stage (at 500 °C), the CO desorption profile was similar, with a gradual decrease until their total desorption.

Table 3
Measurements of hydrogen chemisorption, active superficial centres, catalysts metallic dispersion (DM) and particle diameter, calculated by H₂ chemisorption at 25 °C.

Catalyst	Chemisorbed H ₂ ($\mu\text{mol. g}^{-1}$)	Active superficial centres ($\mu\text{mol}_{\text{Pt}} \text{g}_{\text{cat}}^{-1}$)	D_M (%)	d_p (nm)
PtAc	19.2	38.4	81.4	1.4
PtMgA	10.5	21.1	40.3	2.4
PtSiA	18.1	36.2	81.0	1.4
PtLaA	19.4	38.7	85.9	1.3

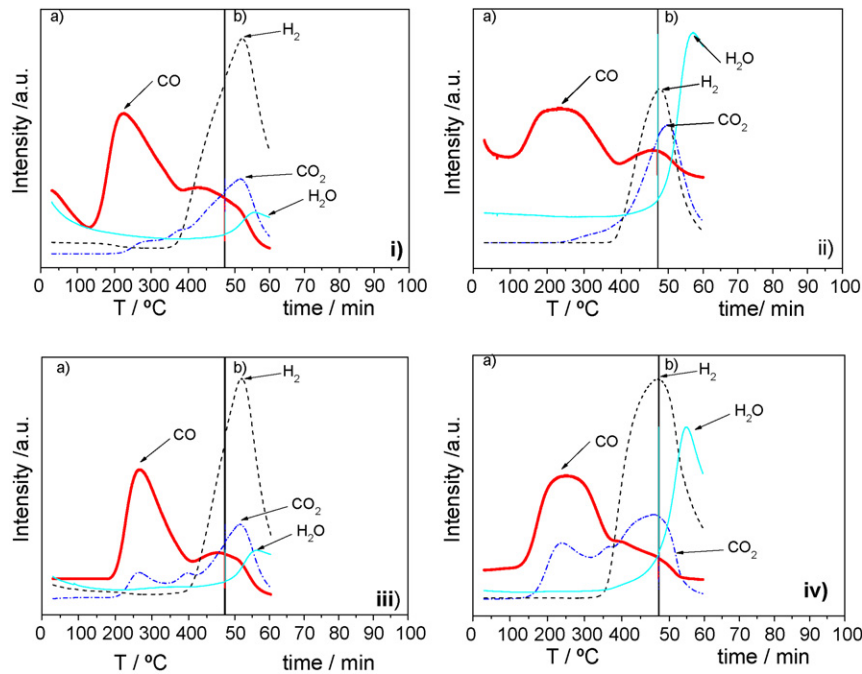


Fig. 2. CO temperature programmed desorption experiments (TPD) performed after the CO adsorption at 25 °C for the catalysts: (i) PtAc, (ii) PtMgA, (iii) PtSiA, (iv) PtLaA.

The CO₂ desorption intensity is a hundred times lower than CO adsorption, due to O₂ was not introduced directly, it came from the oxygen species or from the OH⁻ groups contained within the supports. Nevertheless, it is noteworthy that CO₂ desorption was different for each catalyst. In PtAc, PtSiA y PtLaA catalysts there are three desorption temperatures: 250, 380 and 500 °C, what means that oxygen came from three different species. CO₂ desorption in PtAc, PtSiA and PtMgA catalysts was detected after 200 °C. However, in PtLaA catalyst, the first desorption peak was detected after 140 °C and the CO₂ intensity profile is much higher, what means a greater participation of lattice-oxygen coming from the support in this catalyst. In the isotherm period, a maximum for CO₂ desorption in the first minutes, is observed, decreasing after that.

H₂ desorption took place simultaneously with the CO desorption minimum, located between the high and low temperature peaks. In PtAc y PtSiA catalysts, H₂ desorption was prolonged in the isotherm stage contrary to PtMgA and PtLaA catalysts, in which H₂ desorption was completed when the heating ramp finished. This fact is associated with the presence of less acid centres (OH⁻) in PtMgA and PtLaA catalysts and to their higher reactivity, what is justified by the lower temperature at which H₂ begins to desorb. In PtLaA catalyst, the desorption occurred after 350 °C, while for PtMgA, PtAc and PtSiA catalysts it was necessary to increase the temperature up to 380–400 °C, approximately.

In PtAc and PtSiA catalysts, a slightly H₂O desorption happened after 5 min of the isotherm period. However, in PtMgA and PtLaA catalysts, the H₂O desorption in the isotherm period had a significant intensity. In PtLaA catalyst, it also takes place at 350 °C. H₂O desorption, in a higher quantity and a lower temperature, was due to the higher reactivity of OH⁻ groups, contained in the lowest acidity supports (MgA and LaA).

From the CO TPD test we can conclude that, in O₂ absence, the chemisorbed CO can react with the oxygen that comes from lattice or with OH⁻ groups contained in the support, producing CO₂. At temperatures lower than 400 °C, the two CO₂ desorption peaks probably comes from the reaction between CO and the oxygen of the support. Two types of Pt centres which can be ascribed to these desorption peaks, were observed in PtAc and PtSiA and with more relevance in PtLaA catalyst.

At around 500 °C, the reaction between CO and OH⁻ groups is favoured to produce CO₂ and H₂ simultaneously, what can be explained due to CO₂ desorption and H₂ desorption took place simultaneously.

3.2. Reaction results

The evolution of CO conversion vs. temperature for each of the catalysts considered is shown in Fig. 3. For all the catalysts studied, CO conversions higher than 99% were obtained. It is remarkable that PtLaA catalyst showed a different behaviour compared with PtAc, PtMgA and PtSiA catalysts. On one hand, in these catalysts CO conversion increased until a certain temperature and after that decreased. On the other hand, the stability of CO conversion in PtLaA catalyst between 165 and 255 °C, indicates that CO adsorption does not depend on temperature, what may be due to CO and O₂ adsorption are taking place in different types of centres, without diffusion problems over the catalysts surface.

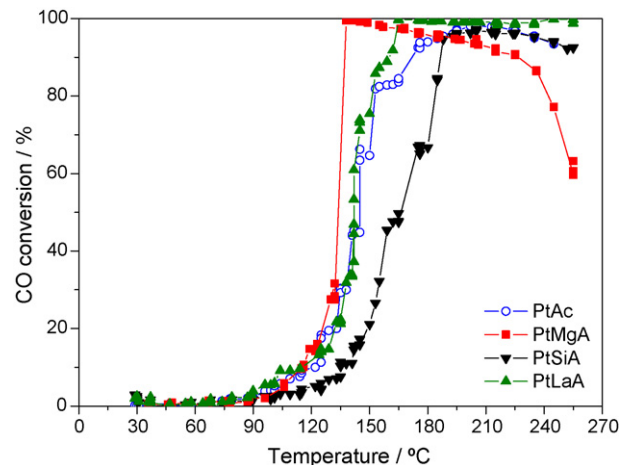


Fig. 3. Evolution of CO conversion as a function of the reaction temperature for (of) PtAc (○), PtMgA (■), PtSiA (▼), PtLaA (▲) catalysts.

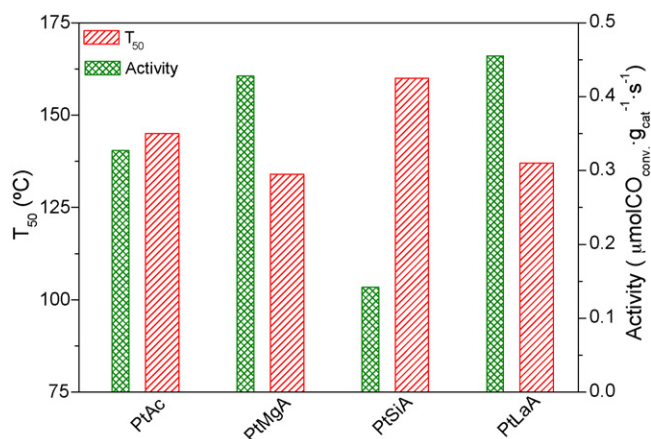


Fig. 4. Temperature needed to achieve a CO conversion of 50% (T_{50}) and catalytic activity of PtAc, PtMgA, PtSiA, PtLaA catalysts.

The light-off temperature or T_{50} , defined as the temperature necessary to achieve a CO conversion of 50%, was different for each of the catalysts considered, being the order PtMgA < PtLaA < PtAc < PtSiA (Fig. 4). The addition of alkaline metals over Al_2O_3 supports modified the interaction between CO and Pt [11], due to the increase in the electronic density, resulting from the electronic transference from the alkaline metal to Pt. One of the supports used in this work was MgA which composition is 50% of MgO and 50% of Al_2O_3 . MgO decreases Al_2O_3 acidity as the results obtained by the acidity test confirmed and as Cho *et al.* reported [11]. This fact led to an increase in the catalyst activity because it seems that at higher temperatures, OH^- groups coming from the support react with CO forming hydrocarbonils, O_2 is adsorbed dissociatively over Pt which has a high electronic density and reacts with the hydrocarbonils forming CO_2 [26]. This fact was confirmed in the TPD test, where from 300 °C CO_2 was detected simultaneously with H_2 , due to the reaction between OH^- groups and the adsorbed CO, leading to both products.

The catalytic activity was estimated in order to compare each of the catalyst considered (Fig. 4). It was calculated as the CO mol converted per unit of time and catalyst weight, at a certain temperature. It followed the order: PtSiA \ll PtAc < PtMgA < PtLaA. Some authors affirm that although La_2O_3 does not modify the reaction mechanism, it increases the concentration of the active catalytic sites on the surface [17]. However, as a consequence of our results, we can conclude that La_2O_3 do modify the reaction mechanism, promoting the CO adsorption. In literature, some tests that can corroborate our results can be found, as for example measurements of the initial adsorption enthalpies of NH_3 over Al_2O_3 and La_2O_3 - Al_2O_3 , using NH_3 microcalorimetric adsorption techniques [27]. Zou *et al.* used an alumina support modified with 10% of La_2O_3 . The results (measured at 150 °C) showed that at low levels of NH_3 coverage ($<50 \mu\text{mol g}^{-1}$), the initial adsorption enthalpies were 125 kJ mol^{-1} in the case of Al_2O_3 and 103 kJ mol^{-1} for $\text{La}_2\text{O}_3/\text{Al}_2\text{O}_3$. So, the decrease in the adsorption enthalpies is directly related to the decrease in the acidity. The addition of La_2O_3 to the support decreases the CO adsorption enthalpy and consequently it increases the reactivity.

Comparing PtLaA and PtAc catalysts, we observe that T_{50} for PtLaA catalyst was lower than for PtAc catalyst, therefore the catalytic activity was higher. In PtLaA catalyst, CO conversion was favoured at low temperatures, because it was not necessary to desorb CO in order to leave enough surface centres for O_2 adsorption. Comparing their TPD profiles (Fig. 2i and iv), we can see a remarkable increase in the intensity of the first peak ascribed to CO_2 desorption (235 °C) in PtLaA with respect to PtAc catalyst (275 °C).

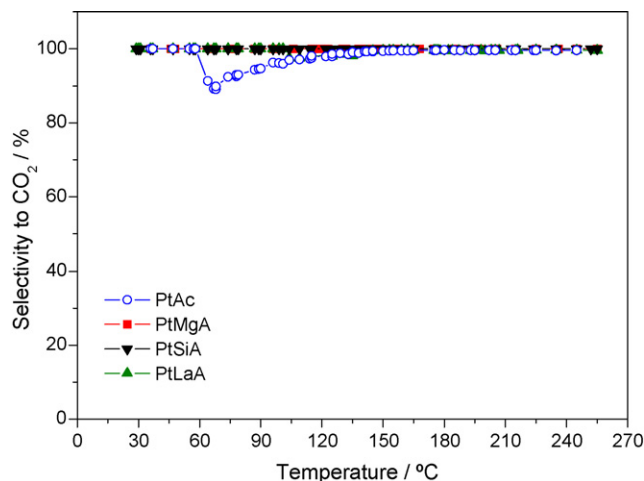


Fig. 5. Evolution of CO_2 selectivity as a function of the reaction temperature of PtAc (○), PtMgA (■), PtSiA (▼), PtLaA (▲) catalysts.

This fact can be connected with the different CO adsorption mechanism involved in each of these catalysts. CO adsorption depends on the support acidity (Table 2), leading to the formation of different species in the catalyst surface. In La_2O_3 presence, carbonated species (bidentate carbonates) are formed, which is in keeping with the results obtained by Martin and Duprez [28]. They studied the surface oxygen mobility in different oxides used as supports and they correlated them. Their results showed that the oxides that showed higher surface acidity practically did not show oxygen mobility. Consequently, in PtLaA catalyst, whose support has a lower surface acidity than PtAc catalyst, the bidentate carbonates formation is favoured. These species can be responsible for the different ways of CO adsorption, overcoming the limitations in CO and O_2 adsorption and favouring a high activity at low reaction temperatures.

O_2 conversion behaves similarly to CO conversion up to 150 °C, when the profile changes completely, being the O_2 conversion practically total.

The selectivity to CO_2 between 25 and 255 °C (Fig. 5) was next to 100% in all the catalysts considered, which shows that oxygen was converted into CO_2 selectively. In PtAc catalyst, from 65 to 115 °C, a decrease in the selectivity to CO_2 was observed. This fact can be explained by the residual H_2 oxidation that remained chemisorbed in the catalyst support since the reduction stage.

Considering these results obtained in the conditions previously reported, we can affirm that PtAc, PtLaA, PtSiA and PtMgA catalysts are highly selective to CO preferential oxidation, since selectivity to H_2O is negligible.

4. Conclusions

The great influence of the support on the activity and selectivity of the catalyst has been proved in this work. The presence of basic oxides in the support, as MgO and La_2O_3 , decreases the surface acidity, what facilitate the PtO_x reducibility leading to a decrease in the catalyst light-off temperature and an increase in the catalytic activity.

In O_2 absence, CO_2 desorption took place in PtLaA catalyst even at low temperatures, what indicates that in La_2O_3 presence, the reaction mechanism differs from PtAc, PtMgA and PtSiA catalysts. The addition of 3% wt of La_2O_3 on Al_2O_3 , has modified the reaction mechanism in which O_2 and CO do not compete during the adsorption stage, contrary to Langmuir–Hinshelwood mechanism in which it is necessary to increase temperature in order to partially desorb CO for leaving some free sites for the dissociative oxygen

adsorption. PtLaA catalyst shows a completely different behaviour, where CO is not only adsorbed over the Pt active centres, but also over La₂O₃, leading to bidentate carbonates which show a high reactivity at low temperatures. The increase of temperature also produces a partial desorption of the CO adsorbed over Pt, favouring the oxygen adsorption and CO₂ production. In addition, at higher temperatures, CO oxidation is activated with OH⁻ groups producing CO₂ and H₂.

At the light of the results obtained, PtLaA is the catalyst which shows the highest activity and therefore, the lowest light-off temperature, and the highest selectivity in CO preferential oxidation, being the selectivity to H₂O negligible.

References

- [1] G. Avgouropoulos, T. Ioannides, Ch. Papadopoulou, J. Batista, S. Hoecer, H.K. Matrilis, *Catal. Today* 75 (2005) 157–167.
- [2] Y. Choi, H.G. Stenger, *J. Power Sources* 129 (2) (2004) 246–254.
- [3] A. Martinez-Arias, A.B. Hungria, M. Fernández-García, J.C. Conesa, G. Munuera, *J. Power Sources* 151 (2005) 32–42.
- [4] Y. Liu, Q. Fu, M.F. Stephanopoulos, *Catal. Today* 93–95 (2004) 241–246.
- [5] F. Mariño, Cl. Descorme, D. Duprez, *Appl. Catal. B: Environ.* 54 (2004) 59–66.
- [6] D.J. Suh, Ch. Kwak, J.-H. Kim, S. Mann Kwon, T.-J. Park, *J. Power Sources* 142 (2005) 70–74.
- [7] M.M. Schubert, A. Venugopal, M. Kahlich, V. Plazk, R.J. Behm, *J. Catal.* 222 (2004) 32–40.
- [8] M.M. Schubert, V. Plazk, J. Garcke, R.J. Behm, *Catal. Lett.* 76 (3–4) (2001) 143–150.
- [9] A. Luengnaruemitchai, S. Osuwan, E. Gulari, *Int. J. Hydrogen Energy* 29 (2004) 429–435.
- [10] M.M. Schubert, A. Venugopal, M.J. Kahlich, V. Plazk, R.J. Behm, *J. Catal.* 222 (2004) 32–40.
- [11] S.H. Cho, J.S. Park, S.H. Choi, S.H. Kim, *J. Power Sources* 156 (2006) 260–266.
- [12] M. Benito, R. Padilla, L. Daza, *ES Patent* 03286 (December 27, 2006).
- [13] M. Bettman, R.E. Chase, k. Otto, W.H. Weber, *J. Catal.* 117 (1989) 447–454.
- [14] M.T. Tiernan, O.E. Finlayson, *Appl. Catal. B: Environ.* 19 (1998) 23–35.
- [15] S. Damyanova, J.M.C. Bueno, *Appl. Catal. A: Gen.* 253 (2003) 135–150.
- [16] F. Domínguez, E. Choren, J. Sánchez, G. Arteaga, *Ciencia* 13 (2005) 103–112.
- [17] N.R.E. Radwan, *Appl. Catal. A: Gen.* 257 (2004) 177–191.
- [18] M. Ferrandon, E. Björnbohm, *J. Catal.* 200 (2001) 148–159.
- [19] P. Thormählen, M. Skoglundh, E. Fridell, B. Andersson, *J. Catal.* 188 (1999) 300–310.
- [20] V. Matolín, I. Matolinova, F. Sutara, K. Veltruska, *Surf. Sci.* 566–568 (2004) 1093–1096.
- [21] R.K. Herz, D.F. Mc Cready, *J. Catal.* 81 (1983) 358–368.
- [22] R.J. Mukerji, A.S. Bolina, W.A. Brown, *Surf. Sci.* 527 (2003) 198–208.
- [23] V.H. Sandoval, C.E. Gigolo, *Appl. Catal. A: Gen.* 148 (1996) 81–96.
- [24] V. Nehasil, I. Stara, V. Matolin, *Surf. Sci.* 331–333 (1995) 105–109.
- [25] R.F. Hicks, Q. Yen, A.T. Bell, *J. Catal.* 89 (1984) 498–510.
- [26] C.K. Costello, M.C. Kung, H.S. Oh, Y. Wang, H.H. Kung, *Appl. Catal. A: Gen.* 232 (2002) 159–168.
- [27] H. Zou, X. Ge, J. Shen, *Thermochim. Acta* 397 (2003) 81–86.
- [28] D. Martin, D. Duprez, *J. Phys. Chem.* 100 (1996) 9429–9438.